JOURNAL OF CATALYSIS **167,** 438–446 (1997)
ARTICLE NO. CA971584

Cracking Behavior of Zeolites with Connected 12- and 10-Member Ring Channels: The Influence of Pore Structure on Product Distribution

A. Corma,[1] M. Davis,* V. Fornés, V. González-Alfaro,† R. Lobo,* and A. V. Orchillés†

*Instituto de Tecnología Química (U.P.V.-C.S.I.C.), Universidad Politécnica de Valencia, Avda. de los Naranjos, s/n, 46022 Valencia, Spain; *Chemical Engineering, California Institute of Technology, Pasadena, CA 91125; and †Departamento de Ingeniería Química, Universidad de Valencia, c/Dr. Moliner 50, 46100, Burjassot (Valencia), Spain*

Received April 22, 1996; revised December 3, 1996; accepted December 23, 1996

***n*-Heptane has been cracked on a CIT-1 zeolite which has connected 12- and 10-member ring (MR) channels, and its behavior was compared with that of MCM-22 with nonconnected 12- and 10-MR channels, and SSZ-24 and BETA with unidirectional and tridirectional 12-MR channels, respectively. The kinetic rate constant is highest for CIT-1, and the decay constant is lowest. From the selectivity point of view, its behavior can be better represented by a system with large cavities (the intersections between the 12- and 10-MR) connected by windows. This gives a behavior typical of that of large pore zeolites. CIT-1 produces a remarkably high selectivity to *i*-C_4, and specially to isobutane. This zeolite shows promise as an additive in FCC operations.**

INTRODUCTION

Among the different types of solid acid catalysts, zeolites have proven to be particularly useful for carrying out catalytic transformation of hydrocarbons of commercial interest in the fields of oil refining, petrochemistry, and chemical production. One reason for their success is the possibility of modulating the Brønsted acid strength which then can be adapted to the acidity needed for a particular reaction. While the control of the surface acidity is important, even more important in the case of zeolites is the possibility of controlling product selectivity by an adequate dimensionalization of their pores and cavities. These geometrical effects have been covered by the so-called shape selectivity effects in microporous solid catalysts (1, 2). If one adds to the above properties, the fact that zeolites are thermally stable, have high adsorption capacities, and are able to preactivate reactant molecules due to the presence of strong electric fields (3) and electronic confinement effects (4) within the micropores, one can understand their success as acid catalysts.

As was indicated above, changes in size and dimensionality of pores have been quite useful for decreasing product selectivities based on molecular sieve effects and on geometrical restrictions for formation of some transition states leading to undesired products. On these bases, processes such as selective cracking, isodewaxing, aromatic alkylation, and alkylaromatic disproportionations (5–10) have been successfully developed.

Until recently, only structures with either 10- or 12-member ring channels and cavities with either uni- or multidirectional topologies were synthesized. However, it was realized that from a fundamental as well as from an applied point of view, it could be of great interest to synthesize structures containing both 12- and 10-member rings in the same structure. Very recently, zeolite MCM-22 was reported as having both 10- and 12-member ring (MR) channels, but they were independent and molecules cannot go from one channel system to the other (11, 12). Another zeolite, NU-87, has pores with 10- and 12-MR which are connected, but only the 10-MR pores are open to the exterior.

Finally, there are other recently reported structures, such as SSZ-33 (13), SSZ-26 (14), and CIT-1 (15), which have connected 12- and 10-MR channels. There is no doubt that a system of pores like this should present special selectivity features for hydrocarbon reactions, taking into account the expected diffusion peculiarities as well as the geometry of the void spaces generated. In some way they can fill the gap existing between bidirectional 10-MR zeolites such as ZSM-5, unidirectional 12-MR such as SSZ-24, Mordenite, Omega, or L zeolites, and finally tridirectional 12-MR zeolites such as BETA.

In the present work we have studied the catalytic cracking of *n*-heptane on a 12/10-MR zeolite (CIT-1) and the results are compared with those obtained on a zeolite with nonconnected 12- and 10-MR channels such (MCM-22), with those from a 12-MR unidirectional zeolite with a pore diameter very close to that of the 12-MR channels in the CIT-1 sample (SSZ-24), and finally with those of a 12-MR tridirectional zeolite such as BETA. The influence of pore geometry and site density on cracking parameters such as olefin/paraffin, C_2/C_5, C_3/C_4 ratios, propylene, butenes, and branched to unbranched products is discussed.

[1] To whom correspondence should be addressed.

0021-9517/97 $25.00

TABLE 1

Physical Properties of the Zeolites Used in This Study

Catalyst	Si/Al ratio	Crystal size (μm)	Surface area (m^2/g)	Pore volume (N_2) (ccg^1)
CIT-1	44.5	1–3	500	0.20
SSZ-24	295	0.5×3	300	0.12
MCM-22	15	0.38	400	0.17
BETA	16	0.20	600	0.24

EXPERIMENTAL

Materials

Samples of the different zeolites [CIT-1 (15), SSZ-24 (16), MCM-22 (17), and BETA (18)] were synthesized following the procedures described in the literature. CIT-1 the physicochemical characteristics of the zeolites are included in Table 1.

NMR Characterization

Solid state ^{27}Al and ^{29}Si NMR spectra were recorded under magic angle spinning (MAS) at ambient temperature on a Varian VXR-400 WB spectrometer and 104.2 and 79.5 MHz, respectively. The ^{29}Si spectra, both Bloch-decay and cross-polarization from ^{1}H, were recorded with a 5-mm Varian probe. ^{27}Al NMR was measured with a 7-mm Varian probe. The acquisition parameters are given in Table 2. The ^{29}Si spectra were deconvoluted using standard Varian software.

Acidity Measurements

Room-temperature IR spectra were recorded with a Nicolet 710 FT-IR spectrometer from zeolite wafers ($10\ mg \cdot cm^{-2}$) mounted in a vacuum cell. Pretreatment of zeolites was performed in the cell at 673 K and vacuum (10^{-2} Pa) overnight. For the adsorption/desorption studies, pyridine vapor (6×10^2 Pa) was adsorbed onto the zeolite.

TABLE 2

MAS NMR Experimental Conditions

Resonance	Pulse (μs)	Flip angle (rad)	Recycle delay (s)	MAS rate (kHz)
		MAS		
^{27}Al	0.3	$\pi/20$	0.5	7
^{29}Si	4.7	$3\pi/8$	60	5
	$\pi/2$ pulse (μs)	Contact time (ms)		
		CP/MAS		
^{29}Si	6.5	4.0	3	5

The excess of pyridine was removed in vacuum over three consecutive (1 h) periods of heating at 523, 623, and 673 K, each of them followed by IR measurements.

Catalytic Experiments

Catalytic experiments were performed in a fixed-bed glass tubular reactor (30×1.6 cm i.d.) with an independently controlled three-zone heater (19). All reactions were carried out at 723 K and atmospheric pressure. Prior to each experiment the catalyst was purged in the reactor for 15 min with nitrogen at reaction temperature. After that *n*-heptane was pumped through the reactor at a constant rate. The catalyst-to-oil ratios (cat/oil) were varied between 0.00625 and 0.05 $g \cdot g^{-1}$ for CIT-1, 0.025 and 0.1 for MCM-22 catalyst, 0.05 and 0.2 for SSZ-24 zeolite, and 0.0125 and 0.05 for BETA. The cat/oil ratios were different for the four catalysts in order to keep the same range of conversion level. These cat/oil ratios were obtained by changing the amount of catalyst in each case, and feeding a constant weight of *n*-heptane (2.00 g). At each cat/oil ratio, experiments were carried out at times on stream of 64, 160, 319, 638, and 1593 seconds. At the end of each run, the reactor was stripped using N_2 for 10 min ($15\ cc \cdot min^{-1}$). During the duration of the reaction and stripping, the liquid products were collected in a glass receiver located at the exit of the reactor which was refrigerated in a water–ice bath. Meanwhile, the gaseous products were collected in a gas buret by water displacement. After every run, the catalyst was regenerated by passing air through the catalytic bed ($50\ cc \cdot min^{-1}$) at 773 K for 6 h.

Reaction products were analyzed by gas chromatography (GC) in a Hewlett–Packard 5890 II chromatograph. Liquid products were analyzed using a DB-1 capillary column of 60 m connected to a flame ionization detector. Gaseous products were analyzed using a 2-m silica gel plus Porapak Q column and a thermal conductivity detector.

RESULTS AND DISCUSSION

Cracking Activity

The accumulated average conversion at different times on stream and different catalyst-to-oil ratios (20) for the different zeolites are given in Fig. 1. From those values and using a pseudo-first-order kinetic model with a concentration-dependent decay function (21),

$$\frac{\delta X}{\delta (W/F_{AO})} = k_t \frac{(1-X)}{(1+\epsilon X)} \cdot C_{AO} \cdot \varnothing \qquad [1]$$

$$\frac{\delta \varnothing}{\delta t} = -K_{md} \cdot \varnothing^m \cdot X \qquad [2]$$

$$X = \frac{1}{t_f} \cdot \int_0^{t_f} X \cdot dt, \qquad [3]$$

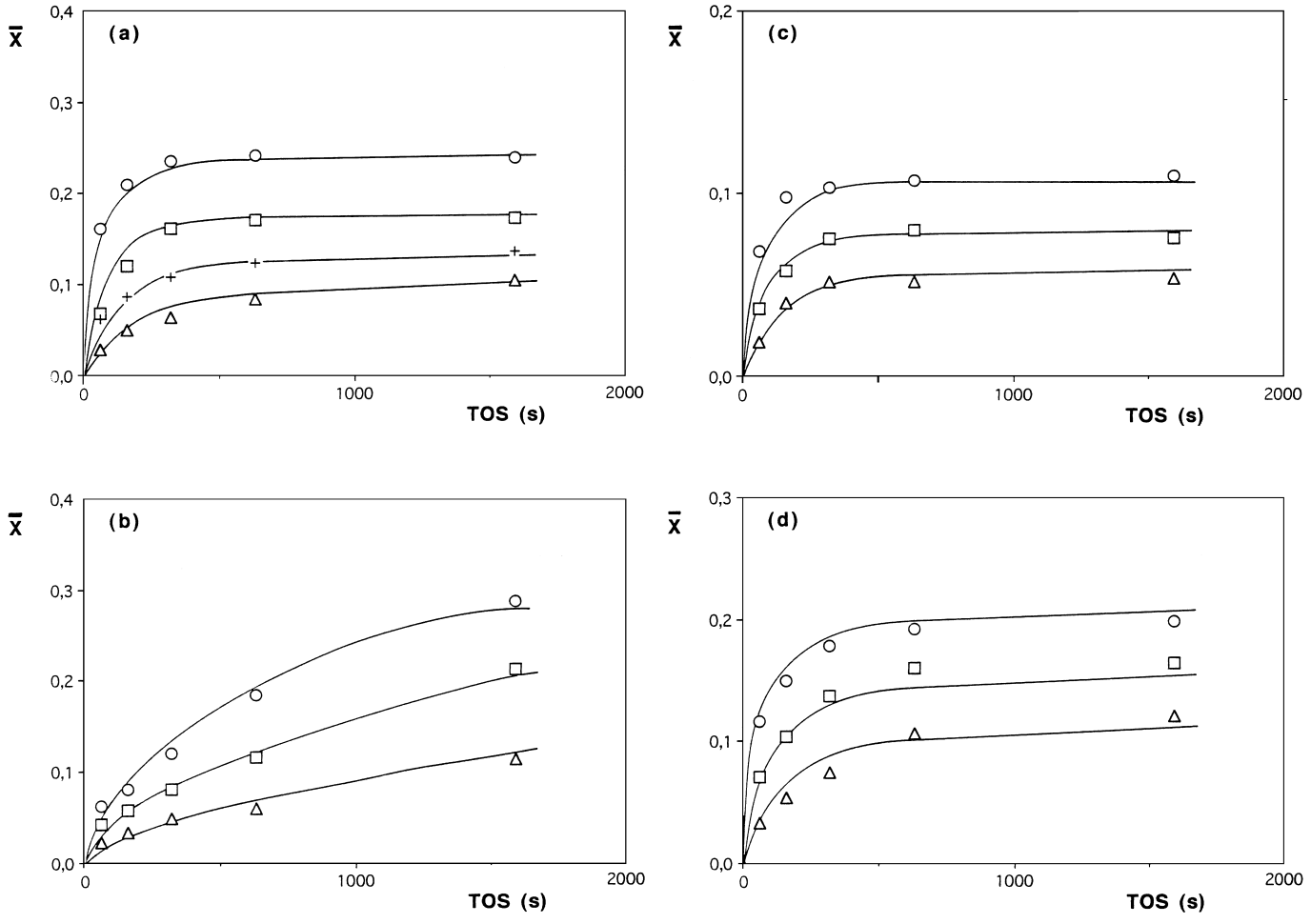

FIG. 1. Experimental and calculated cumulative average conversion for zeolites used in this work. (a) CIT-1 catalyst: (△) 0.00625, (+) 0.01250, (□) 0.02500, (◯) catalyst to oil ratios. (b) MCM-22 catalyst: (△) 0.0250, (□) 0.0500, (◯) 0.1000 catalyst to oil ratios. (c) SSZ-24 catalyst: (△) 0.0500, (□) 0.1000, (◯) 0.2000 catalyst to oil ratios. (d) BETA catalyst: (△) 0.0125, (□) 0.0250, (◯) 0.0500, catalyst to oil ratios. Continuous lines are the fitted curves.

the parameters k_t, K_{md}, and m have been obtained and are given in Table 3. Parameter k_t is directly proportional to the kinetic rate constant and therefore can be used to compare the catalytic activity of the different zeolite catalysts. From the results given in Table 3, it can be seen that CIT-1 zeolite is the most active catalyst, followed by zeolite BETA, MCM-22, and finally SSZ-24. Taking into account that *n*-heptane can easily diffuse in these structures (22), differences in activity cannot be related with geometrical factors but rather to the number and strength of the acid sites. Thus, we have calculated the activity per Al site by dividing parameter k_t by the ratio Al/Al + Si. The results, given in Table 3, indicate that the activity per site is much larger in the CIT-1 and SSZ-24 zeolites. However, the above calculation presupposes that all Al in the zeolite is in framework positions, something that it is not necessarily true. Thus we have checked if all the Al was in a tetrahedral coordination, and the results from ^{27}Al MAS NMR (Fig. 2) clearly show that there part of Al is in an octahedral coordination; consequently, we cannot calculate the activity per framework Al by dividing the kinetic rate constant by the total Al content of the zeolite. In a second step, we have carried out the analysis of the samples by ^{29}Si MAS NMR (Fig. 3) and from this the framework Si/Al ratios have been calculated

TABLE 3

Kinetic and Decay Parameters in Zeolites Used in This Study

	Catalyst			
	CIT-1	MCM-22	SSZ-24	BETA
k_t ($m^3 \cdot s^{-1} \cdot kg^{-1}$)	4.02×10^{-2}	7.61×10^{-3}	4.41×10^{-3}	2.73×10^{-2}
k_{md}	0.1532	2.2539	0.4113	0.1703
m	1.8913	4.2886	1.9376	2.0404
k_t/(Al/(Al + Si)) ($m^3 \cdot s^{-1} \cdot kg^{-1}$)	1.8290	0.1218	1.3050	0.4368
$k_t/Al^{IV}/Al^{IV} + Si$ ($m^3 \cdot s^{-1}.kg^{-1}$)	2.25	0.139	1.50	0.6306

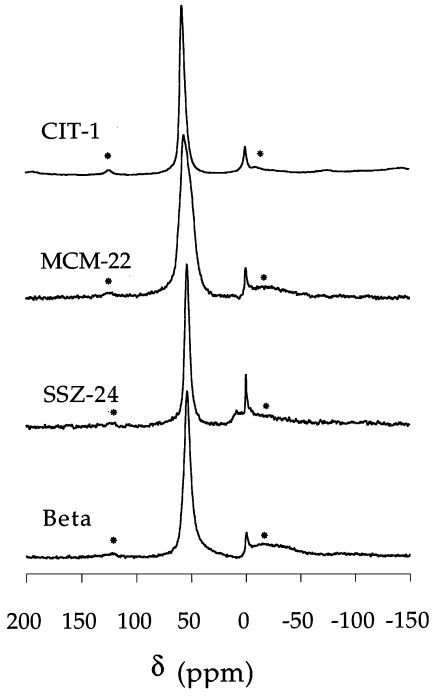

FIG. 2. ^{27}Al MAS NMR spectra. The asterisks indicate spinning sidebands.

(Table 4). However, it should be taken into account that these values will also be approximations, since situations involving one Si bonded to three Si and one hydroxyl are not separated from those with three Si and one Al. In order to see if we have, in this case, connectivity defects which can lead to the above situation, cross polarization from H^+ to Si has been done (Fig. 3), and the results show that there are Si with three Si and one OH which will be responssible for an underestimation of the framework Si/Al ratio. Due to this we have calculated the ratio of Al^{IV}/Al^{VI} from the ^{27}Al MAS NMR spectra, considering that by having the samples saturated with water all the Al^{VI} is NMR-visible. From these values the resultant framework Si/Al ratios have been calculated, and the results are given in the last column of Table 4. From these, the activity per framework Al has been calculated and the results are given in Table 3. In order to explain the higher intrinsic cracking activity of the 12/10-MR zeolite we have measured the population of the bridgingOH group and the number of Brønsted acid sites able to retain pyridine at different desorption temperatures. The results in Fig. 4 clearly indicate that the CIT sample has two bands at ~3620 and ~3525 cm^{-1} that can be named high- (HF) and low-frequency (LF) bands, respectively. The presence of HF and LF hydroxyls have been observed in other

TABLE 4

Calculated Framework Si/Al Ratios from NMR Data

Sample	Si/Al (from ^{29}Si)	Si/Al (from Al^{IV}/Al^{VI})
CIT-1	21.0	55
SSZ-24	58.0	38.4
MCM-22	17.6	17.3
BETA	14.6	22.1

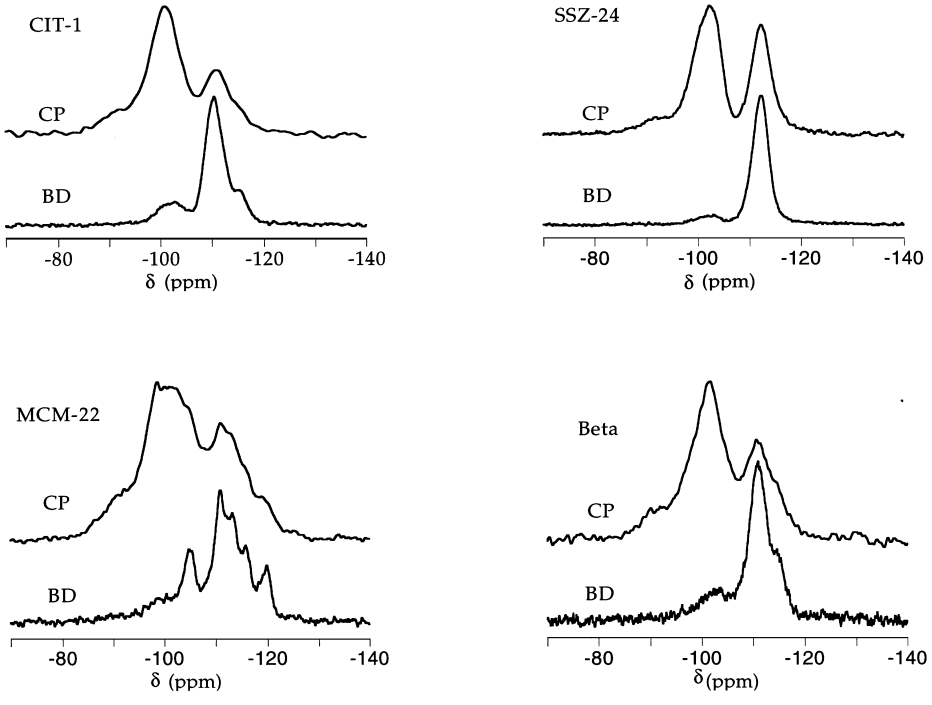

FIG. 3. Bloch-decay (BD) and cross polarization (CP) ^{29}Si MAS NMR spectra.

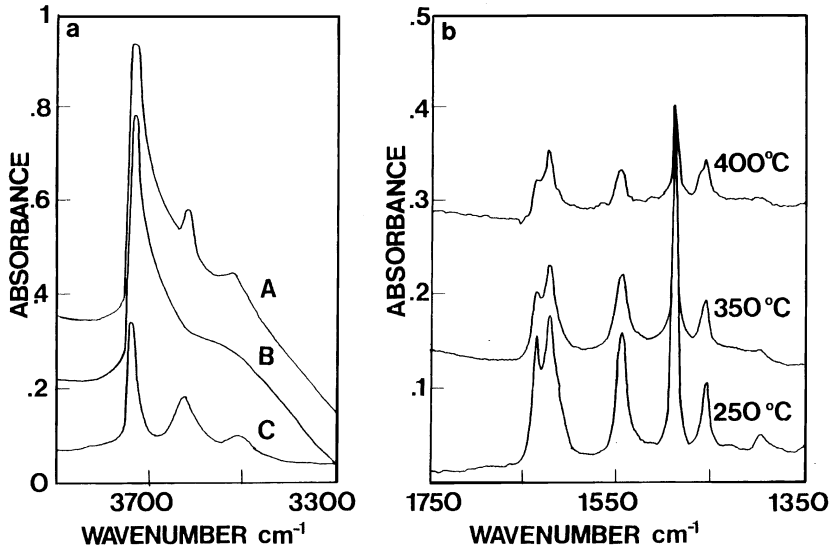

FIG. 4. Infrared spectra of CIT-1. Hydroxyl region (A) before adsorbing pyridine, and (B) after pyridine adsorption and desorption at 250°C. (C) Difference spectra (A-B). Infrared spectra of the adsorbed pyridine, after desorption at 250, 350, and 400°C.

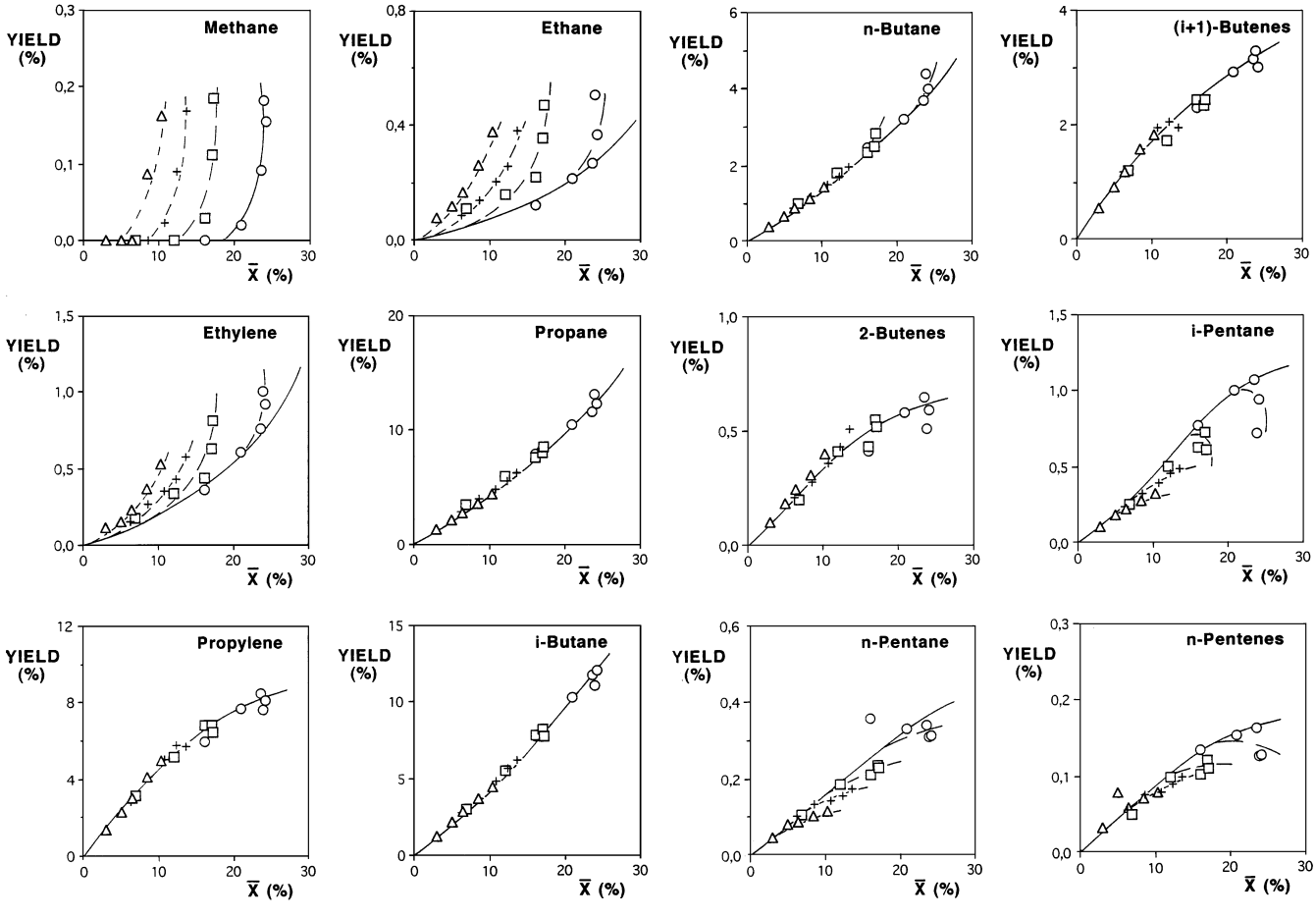

FIG. 5. Selectivity plots for *n*-heptane cracking over CIT-1 zeolite. Experimental points: (△) 0.00625, (+) 0.01250, (□) 0.02500, (○) 0.05000 catalyst to oil ratios. Continuous lines are the OPE curves.

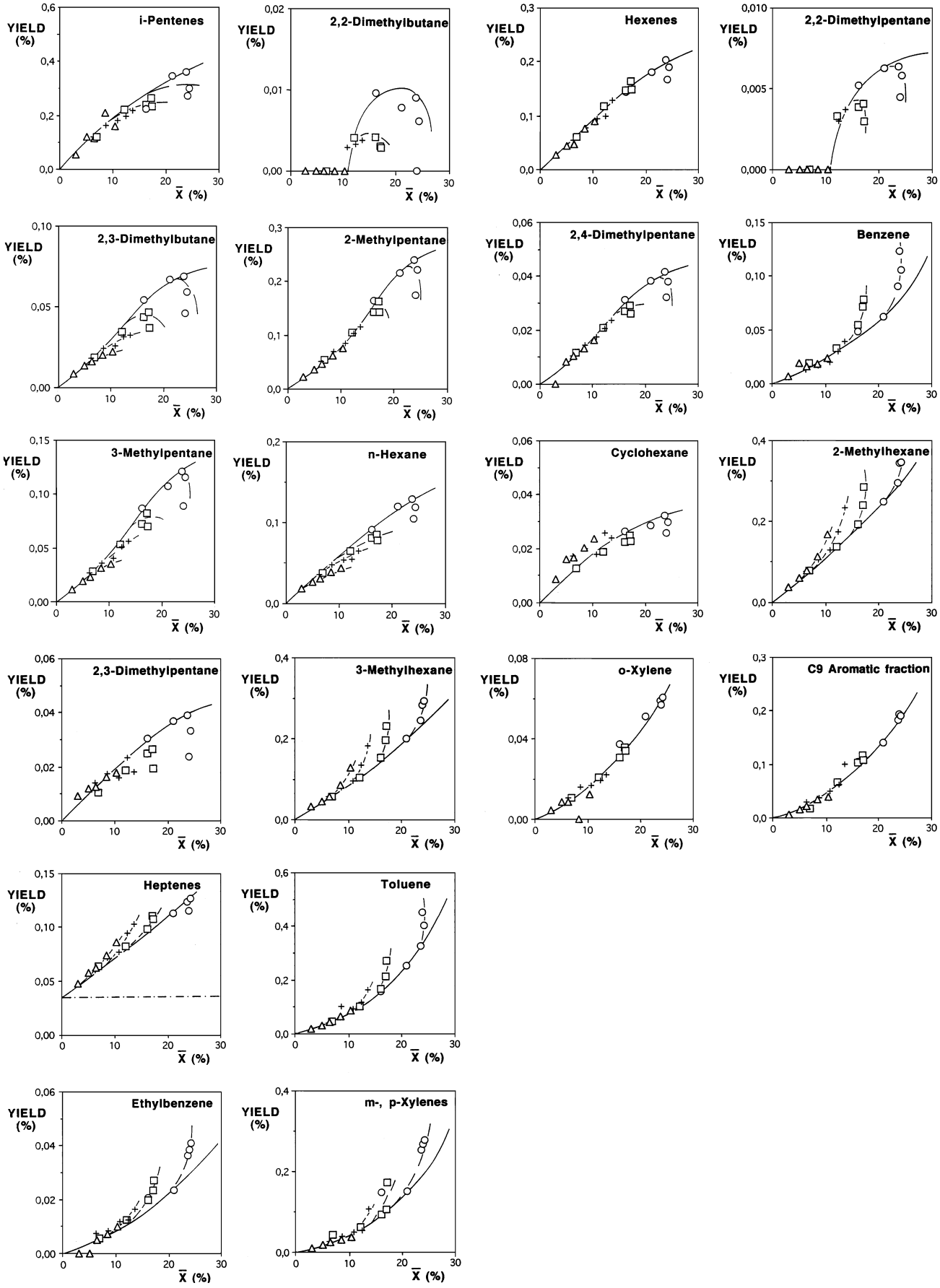

FIG. 5—*Continued*

zeolites and zeotypes such as faujasite (23), SAPO 37 (24), SAPO-5 (25), and SAPO-40 (26), and assigned to Brønsted OH groups located in large pores or cavities (HF), and in small cavities, in side pockets, and/or in a pseudo H-bonding interaction with neighboring oxygen atoms (LF). If this is so, and taking into account that CIT-1 has no small cavities, one could hypothesize that the low-frequency band could be related to hydroxyls in which the H is in some type of side pocket, or interacting with neighboring oxygen atoms through a pseudo H-bonding type of interaction.

Concerning the strength of the acid sites, the IR spectra in the pyridine region taken after desorption at increasing temperatures (Fig. 4) clearly show that CIT-1 still has a large amount of very strong acid sites, i.e., those retaining pyridine at 673 K desorption temperature. The presence of very strong acid sites in the case of CIT-1 zeolite can explain the larger activity per site shown by this zeolite.

Catalyst Decay

The decay parameters obtained for the different zeolites are given in Table 3. Similar decay orders are obtained in samples CIT-1, SSZ-24, and BETA, and the values indicate that a second-order decay with respect to the concentration of active sites exists. The deactivation order for MCM-22 indicates a different mechanism for deactivation, and the value is similar to that in a 10-MR system such as MFI. With respect to the decay constant, very similar values are found for CIT-1 and BETA; the value for SSZ-24 is higher, indicating that SSZ-24 decays faster that BETA and CIT-1 zeolites. This is in keeping with the fact that smaller amounts of coke are formed on the BETA and CIT-1 zeolites; moreover, coke has a more deletorious effect on unidirectional zeolites due to pore pluging.

Cracking Selectivity

Pure hydrocarbons have been used extensively to compare the cracking activity of zeolite catalysts (27); it was thought that the ranking obtained could be extrapolated to the results one would obtain when carrying out the catalytic cracking of gas/oil, and therefore that their relative activity in FCC could be predicted. Unfortunately this was proven not to be the case (28), and it was concluded that pure hydrocarbons could not be used to predict the relative FCC activity of a series of zeolite catalysts. On the other hand it was found (30) that the tendencies in selectivity features observed with pure compounds can be extrapolated quite well to the case of gas/oil feeds. Indeed, when *n*-paraffins and cycloalkanes, such as *n*-heptane and methylcyclohexane, are used as model compounds, selectivity parameters such as olefin/paraffin, C_2/C_5, C_3/C_4, CMR (Cracking mechanism ratio), *i*-C_4/*n*-C_4, and *i*-C_5/*n*-C_5 can be used to characterize the reactivity behavior of the catalysts from the point of view of their ability to catalyze hydrogen transfer reactions, to produce dry gas, and in a more general way to produce more or less protolytic cracking with respect to β-scission. Taking these parameters into account, one should be able to predict which catalyst can produce more olefins and less $C_1 + C_2$ in the gas fraction and a higher research octane number (RON) in the gasoline (33).

In our case, full selectivity curves for all products obtained during cracking of *n*-heptane on CIT-1 are given in Fig. 4. From the shape of the curves it can be said that the primary and secondary products obtained on CIT-1 are those expected from a large-pore zeolite.

From the selectivity curves and considering the primary products, one can calculate the initial selectivities, and the values obtained for all catalysts are given in Table 5. The selectivity behavior of the different zeolites studied here certainly can be discussed on the basis of these values. However, we find it more relevant, to compare their performance on the basis of a series of selected parameters which give direct information not only on the cracking mechanisms involved, but also as yard sticks to predict, on a com-

TABLE 5

Initial Selectivities Calculated by Measuring the Slope at Origin in Fig. 5

Product	Catalyst			
	CIT-1	MCM-22	SSZ-24	BETA
Methane	—	—	—	0.0020
Ethane	0.0078	0.0346	0.0020	0.0039
Ethylene	0.0226	0.0558	0.0465	0.0507
Propane	0.4127	0.4068	0.3639	0.4712
Propylene	0.4538	0.5063	0.5400	0.4270
i-Butane	0.4100	0.3716	0.4856	0.3201
$(i+1)$-Butenes	0.1637	0.2454	0.2098	0.2035
n-Butane	0.1335	0.1573	0.1026	0.1812
2-Butenes	0.0305	0.0487	0.0354	0.0481
i-Pentane	0.0361	0.0330	0.0424	0.0440
n-Pentane	0.0155	0.0148	0.0095	0.0273
n-Pentenes	0.0067	0.0119	0.0071	0.0117
i-Pentenes	0.0171	0.0264	0.0164	0.0267
2,3-Dimethylbutane	0.0028	0.0019	0.0032	0.0018
2-Methylpentane	0.0077	0.0050	0.0052	0.0064
3-Methylpentane	0.0042	0.0024	0.0031	0.0027
n-Hexane	0.0057	0.0044	0.0034	0.0105
Hexenes	0.0900	0.0081	0.0082	0.0084
2,4-Dimethylpentane	0.0017	—	0.0020	0.0016
Benzene	0.0024	0.0030	0.0016	0.0009
Cyclohexane	0.0019	0.0017	0.0021	0.0025
2-Methylhexane	0.0117	0.0113	0.0133	0.0165
2,3-Dimethylpentane	0.0019	—	0.0035	0.0011
3-Methylhexane	0.0087	0.0046	0.0082	0.0091
Heptenes	0.0037	0.0024	0.0055	0.0054
Toluene	0.0063	0.0061	0.0048	0.0063
Ethylbenzene	0.0008	—	—	0.0008
m^-, *p*-Xylene	0.0040	0.0023	0.0022	0.0064
o-Xylene	0.0015	—	—	0.0017
C9 aromatic fraction	0.0030	—	0.0030	0.0059

TABLE 6

Parameters Selected to Compare the Behavior of Different Zeolites

Ratio	Catalyst			
	CIT-1	MCM-22	SSZ-24	BETA
Alkene/alkane	0.76	0.87	0.85	0.72
C_3/C_4	1.17	1.11	1.08	1.19
i-C_4/total C_4	0.56	0.45	0.58	0.43
i-C_4/n-C_4	3.07	2.36	4.74	1.77
i-C_5/n-C_5	2.33	2.24	4.44	1.61
$(C_1+C_2)/i$-C_4	0.07	0.24	0.10	0.18

parative basis, the behavior of these zeolites when used as cracking catalysts or additives during gas/oil cracking in FCC operations. The parameters considered and the values obtained are given in Table 6. The olefin/paraffin ratio obtained on the bases of initial selectivities follows the order MCM-22 > SSZ-24 > CIT-1 > BETA. In the three large-pore zeolites, i.e., SSZ-24, CIT-1, and BETA, the differences should not be very large, and since in this case there are no geometrical restrictions for bimolecular reactions to occur, we relate those differences with the different framework Si/Al ratio of samples. Indeed SSZ-24 has the largest framework Si/Al ratio, followed by CIT-1 and BETA (Tables 1 and 4). This will show that from this point of view the presence of 10-MR in CIT-1 has practically no influence on catalytic behavior, indicating that the catalytic behavior of this zeolite can be explained better by considering a series of large void spaces formed in the crossing point of the 12- and 10-MR channels; communication between these spaces occurs by way of 10- and 12-MR windows (30). However, in the case of MCM-22 with a lower Si/Al ratio, a larger olefin/paraffin ratio is obtained due to the presence of the independent 10-MR channel system which presents sterical hindrance for hydrogen transfer reactions to occur.

The C_3/C_4 ratio shown by the zeolites is typical of large-pore zeolites, and only the value for the SSZ-24 sample is lower than expected. In the case of MCM-22 the behavior is between that of 10- and 12-MR zeolites (12).

However, what really establishes a large difference between the zeolites is either the ratio of i-C_4 to total C_4 or the ratios i-C_4/n-C_4 and i-C_5/n-C_5. All three ratios are much higher on SSZ-24 and CIT-1 zeolites. From a mechanistic point of view, one can expect the i-C_4 to be formed mainly by β-scission of the bulky 2,2′-dimethylpentane and 2,4-dimethylpentane carbenium ions. If this is so, one could, in principle, correlate the ratio of i-C_4 to total C_4 with the diameter of existing void space, i.e., diameter of the channel in unidirectional zeolite, diameter of the void space generated in the crossing point of intersecting channels in multidirectional zeolites, and the diameter of zeolite cavities when they exist. Indeed, when i-C_4/total C_4 is plotted versus zeolite internal free space for a series of zeolites, a good correlation with this parameter is observed (Fig. 4). In the same curve it can be seen that both CIT-1 and SSZ-24 fall well above the curve, and consequently well above any of the previously tested zeolites. To explain these results, one would have to assume that the β-scission plus hydride transfer mechanism is more favored with respect to protolytic cracking on CIT-1 and SSZ-24 than on BETA zeolite.

In order to verify this, we have calculated the cracking mechanism ratio of the above zeolites. The cracking mechanism ratio (29) (CMR), given as the ratio of C_1+C_2/i-C_4, is a useful parameter to show the relative importance of protolytic versus β-scission cracking. The larger the CMR value, the larger the ratio of protolytic to β-scission cracking. Taking this into account and from the values given in Table 5, it is clear that the contribution of β-scission is much larger in the case of CIT-1 and SSZ-24 than in the case of BETA zeolite. This is even more true if one takes into account that CIT-1 and SSZ-24 have larger framework Si/Al ratios than BETA zeolite; it is known that the higher the framework Si/Al ratio, the larger the ratio protolytic/β-scission.

As was said above, isobutane can be formed by cracking of 2,2′-Dimethylpentane followed by hydride transfer, and also by hydrogenation of isobutene via hydrogen transfer, as can be deduced from the unstable character of isobutene shown in the corresponding selectivity curve. When the ratio of isobutane to isobutene has been calculated from the initial selectivities, it can be seen that this ratio is much larger for CIT-1 and SSZ-24 than for BETA and MCM-22

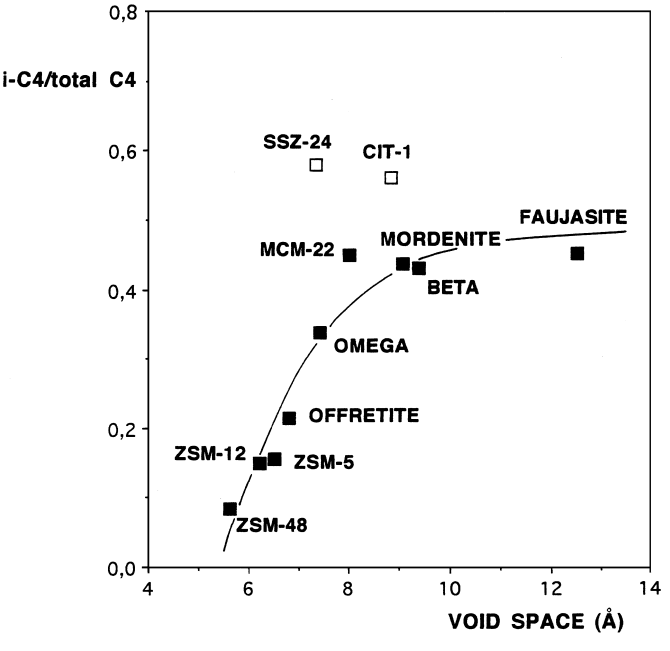

FIG. 6. Correlation of i-C_4/total C_4 ratio versus void space in a large series of zeolites.

zeolites. We can then conclude that on CIT-1 and SSZ-24 either there is a very selective cracking route through the 2,2′-dimethylpentane carbenium ion, or (more probably) that a fast hydrogen transfer occurs on the two zeolites, converting the isobutene into isobutane; something which is consistent with the observed high contribution of the bimolecular β-scission mechanism. However, this conclusion may be in contradiction with the higher olefin paraffin observed on CIT-1 with respect to Beta zeolite. Thus, we attribute the large contribution of the β-scission mechanism observed on CIT-1 to the fact that this zeolite presents very strong acid sites combined with relatively large available void spaces. The presence of strong acid sites increases the average lifetime of the carbenium type species, and this combined with void spaces large enough to favor the occurrence of bimolecular reactions can be responsible for the observed behavior.

In conclusion, CIT-1 zeolite containing intersecting 10- and 12-MR channels has a large proportion of very strong Brønsted acid sites. CIT-1 presents a very unique cracking behavior when compared with other zeolites. It gives a very high ratio of β-scission to protolytic cracking, producing large ratios of i-C_4/n-C_4 and i-C_5/n-C_5, while at the same time it gives a high ratio of isobutane to isobutene. Due to its particular cracking behavior, this zeolite also produces lower amounts of dry gases ($C_1 + C_2$) and consequently appears as an interesting active component in FCC catalyst formulations. The actual challenge is to synthesize the material by a method inexpensive enough to make it feasible for use as an additive.

ACKNOWLEDGMENTS

The authors thank CICYT, Project MAT 94-0359-C02-01, for financing part of this work.

REFERENCES

1. Csicsery, S. M., *J. Catal.* **100**, 541 (1986).
2. Derouane, E. G., and Gabelica, Z., *J. Catal.* **65**, 486 (1980).
3. Mirodatos, C., and Barthomeuf, D. J., *J. Catal.* **44**, 121 (1989).
4. Corma, A., Zicovich-Wilson, C. M., and Viruela, P., *J. Phys. Chem.* **98**, 10863 (1994).
5. Biswas, J., and Maxwell, I. E., *Appl. Catal.* **63**, 197 (1990).
6. Bennet, R. N., Elkes, G. J., and Waulers, G. J., *Oil Gas J.* **3**, 79 (1975).
7. Dwyer, F. G., Lewis, P. J., and Schneider, F. M., *Chem. Eng.* **83**, 90 (1976).
8. Absil, R. P. L., Ham, S., Leiby, S. M., Marler, D. L., McWilliams, J. P., and Shihabi, P. S., *AlChE Summer Nat. Mtg. Denver* **Aug.**, 21 (1988).
9. Brennan, J. A., Garwood, J. A., Yurchak, S., and Leew, *Proc. Int. Sem. Alternate Fuels 191* (1981).
10. Corma, A., *Catal. Lett.* **22**, 33 (1993).
11. Leonowicz, M. E., Lawton, J. A., Lawton, S. L., and Rubin, M. K., *Science* **264**, 1910 (1994).
12. Corma, A., Corell, C., Martinez, A., Pérez-Pariente, J., *Appl. Catal. A: General* **115**, 121 (1994).
13. Zones, S. L., U.S. Patent 4963337. Chevron Research Co., 1990.
14. Zones, S. L., Santilli, J. N., Ziemer, J. N., Holtermann, D. L., Pecoraro, T. A., and Innes, R. A., PCT/US89/01179, Chevron Research Co., 1989.
15. Lobo, R. F., and Davis, M. E., *J. Am. Chem. Soc.* **117**, 3764 (1995).
16. Van Nordstrand, V. A., Santilli, D. N., and Zones, S. I., *in* "Molecular Sieves: Synthesis of Microporous Materials" (M. L. Occelli and H. Robson, Eds.), p. 373, 1992.
17. Corma, A., Corell, C., and Pérez-Pariente, J., *Zeolites* **15**, 2 (1995).
18. Camblor, M. A., and Pérez-Pariente, J., *Zeolites* **11**, 202 (1991).
19. Corma, A., González Alfaro, V., and Orchilles, A. V., *Appl. Catal. A: General* **129**, 203 (1995).
20. Wojciechowski, B. W., *Catal. Rev. Sci. Eng.* **9**, 79 (1974).
21. Corma, A., Miguel, P. J., and Orchillés, A. V., *J. Catal.* **145**, 56 (1994).
22. Frilette, V. J., Haag, W. O., and Logo, R. M., *J. Catal.* **67**, 218 (1981).
23. Jacobs, P. A., and Uytterhoeven, J. B., *J. Chem. Soc. Faraday Trans.* **1669**, 359 (1973).
24. Dzwiggi, S., Briend, M., Shiholeslami, A., Peltre, M. J., and Barthomeuf, D., *Zeolites* **10**, 57 (1990).
25. Kustov, L. M., Zubkov, S. A., Kazansky, V. B., and Bondar, L. A., *in* "Studies in Surface Science and Catalysis" (P. A. Jacobs *et al.*, Eds.), p. 303. Elsevier, Amsterdam, 1991.
26. Onida, B., Gabelica, Z. G., Laurenço, E., and Garrone, E., *J. Phys. Chem.*, in press.
27. Wojciechovsky, B. W., and Corma, A., "Catalytic Cracking, Catalysts, Chemistry and Kinetics." Marcel Dekker, New York, 1986.
28. Corma, A., and Martínez-Triguero, J., *Appl. Catal. A: General* **118**, 153 (1996).
29. Corma, A., Fornés, V., Martinez, A., Melo, F., and Pallota, O., *in* "Studies in Surface Science and Catalysis" (P. J. Grobet *et al.*, Eds.), Vol. 37, p. 495. Elsevier, Amsterdam, 1988.
30. Corma, A., Miguel, P. J., and Orchillés, A.V., *Appl. Catal. A: General* **117**, 29 (1994).
31. Corma, A., Fornés, V., Melo, F., and Pérez-Pariente, J., *in* "Fluid Catalytic Cracking: Role in Modern Refining" (M. L. Ocelli, Ed.), ACS Symp. Ser., Vol. 375, p. 49. American Chemical Society, Washington, DC, 1988.
32. Corma, A., Fornés, V., Montón, J. B., and Orchillés, A. V., *J. Catal.* **107**, 288 (1987).
33. Zones, S. I., Olmstead, M. M., and Santilli, D. S., *J. Am. Chem. Soc.* **114**, 4195 (1992).
34. Corma, A., and Orchillés, A. V., *J. Catal.* **115**, 551 (1989).
35. Wielers, A. F. H., Waarkamp, M., and Post, M. F. M., *J. Catal.* **127**, 51 (1991).